

Aligned Double-Walled Carbon Nanotube Long Ropes with a Narrow Diameter Distribution

Wencai Ren and Hui-Ming Cheng*

Shenyang National Laboratory for Materials Science, Institute of Metal Research,
Chinese Academy of Sciences, Shenyang 110016, China

Received: November 12, 2004; In Final Form: February 6, 2005

Aligned double-walled carbon nanotube (DWNT) long ropes with a narrow diameter distribution were directly synthesized by sulfur-assisted floating catalytic decomposition of methane. The DWNT ropes are typically up to several centimeters in length and possess good alignment and high purity. High-resolution transmission electron microscopy (HRTEM) images and resonant Raman spectra revealed that the outer and inner tube diameters of the DWNTs are narrowly distributed in the range of 1.7–2.0 and 1.0–1.3 nm, respectively. Moreover, based on the resonant Raman measurements, the electronic properties of the two constituent tubes of the DWNTs were identified. The successful synthesis of such DWNTs opens the possibility for their fundamental studies and further applications as nanomechanical, nanooptical, and nanoelectronic devices.

Introduction

Nanotubes provide an ideal intriguing one-dimensional system suitable for fundamental studies of atomically well-defined materials and have considerable potential for future technological applications.¹ For example, single-walled carbon nanotubes (SWNTs) can be expected to be used as the building blocks of nanoscale electronic devices since they can be either semiconducting or metallic depending on their diameters and chiralities.^{1,2} Although some interesting applications can be explored only in multiwalled carbon nanotubes (MWNTs), the fundamental studies and engineering applications have been still relatively limited because of the difficulty in the synthesis of MWNTs with homogeneity in diameter and shell number.

The double-walled carbon nanotube (DWNT) is a special MWNT only consisting of two coaxial SWNTs, which possesses some unique properties.^{3–5} It is expected to have some potential applications directly as nanoscale devices, due to its special double wall structure, such as a molecular conductive wire or a molecular capacitor in a memory device, depending on the electronic properties of the two constituent tubes.³ Therefore, it is very important to control and identify the diameters and the electronic properties of the two constituent tubes for their promising applications as nanoscale electronic devices.

So far, several methods have been developed to produce DWNTs, such as C₆₀ coalescence inside a suitable SWNT (peapod method),⁶ the hydrogen arc discharge method,⁷ and the CVD method.^{8–10} However, the DWNTs produced by these methods, except for the peapod method, have a wide diameter distribution and large diameter, which becomes the bottleneck for their further studies and applications since some novel properties related to the size effect can be enhanced with smaller tube diameters, and fundamental studies require CNTs with homogeneous diameter or at least narrow diameter distribution. Moreover, two well-known disadvantages of the peapod method (discontinuous inner tube structure and low DWNT content in the product), due to the strict demand for the diameters of the

template SWNTs (1.3–1.6 nm), hindered their studies and applications.

Furthermore, the mechanical, optical, and electronic properties of CNTs can be enhanced, if their aligned long continuous ropes can be synthesized.^{11–13} For some potential applications, all these properties are simultaneously important, which is the motivation for considerable efforts for the synthesis of ordered nanostructures. Such ordered rope structures can be used as strong, high-conducting microcables or as mechanically robust electrochemical microactuators.^{14,15} Moreover, theoretical calculation indicates that the DWNTs possess higher strength per unit area in the nanotube axis direction than SWNTs^{1,16} because of the relatively small cross-section of the hollow core. However, the aligned DWNT long ropes have so far rarely been reported.

Here, we report a direct synthesis method of aligned DWNT long ropes with an inner and outer diameter of 1.0–1.3 and 1.7–2.0 nm, respectively. Moreover, the electronic properties of the two constituent tubes of the DWNTs were identified based on the resonant Raman measurements, and the result indicates that the product consists of some semiconducting-metallic DWNTs.

Experimental Procedures

The synthesis equipment was described in detail in our previous paper.¹⁷ In general, methane was used as the carbon source, hydrogen was used as the carrier gas, ferrocene was used as the catalyst precursor, and thiophene was carried into the reactor by methane to enhance the growth of CNTs. For the aligned DWNT rope growth, the reaction tube was first heated to reach 1373 K in a hydrogen atmosphere. Then, methane (250 sccm) and hydrogen (1800 sccm), accompanied with the catalyst precursor (~0.03 g/min) and thiophene (~8.3 × 10⁻³ g/min), were introduced into the reaction tube for 10 min, followed by cooling the CVD system in hydrogen to room temperature. Macroscopically long DWNT strands or ropes as long as 10 cm were formed during the reaction process, sticking to the thermocouple cover tube and hanging on the tube wall of the reactor. It was worth noting that this method can be used

* Corresponding author. E-mail: cheng@imr.ac.cn.

to synthesize aligned DWNT ropes in a large scale due to the continuous introduction of the carbon source, carrier gas, catalysts, and thiophene.

The obtained strands can be manipulated quite easily because of their macroscopic thickness and length. For example, they can be easily separated to some thin ropes 20 μm in diameter by a pair of tweezers with a sharp tip. The thin rope was employed as samples for direct structural characterizations using scanning electron microscopy (SEM), high-resolution transmission electron microscopy (HRTEM), and Raman spectroscopy (excited by a 632.8 and 514.5 nm laser). To obtain the iron and sulfur contents in the product, thermogravimetric analysis (TGA) and energy-dispersive X-ray spectroscopy (EDX) were also adopted.

To characterize the alignment of the DWNT ropes, polarized Raman measurements were performed at room temperature, which were excited with a He/Ne laser (632.8 nm). A microscope with a 100 \times objective lens was used for focusing the laser beam and collection of the scattered light. All Raman spectra were taken in backscattering configuration, with the incident and scattered light propagating perpendicular to the rope axis. The spectra were recorded with parallel polarization of the incoming and scattered light (VV configuration). In the measurements, the axis of the DWNT rope was carefully rotated manually to ensure that the laser signals were from almost the same spot of a thin DWNT rope, and the angles (θ) between the axis of the rope and the polarization direction of the incident laser were calculated from the optical microimages obtained from a digital camera, with an accuracy of $\pm 2^\circ$.

Results and Discussion

After a 10 min synthesis, some ropes up to 10 cm were formed, sticking to the thermocouple cover tube. Two characteristics were found for the product. First, the DWNTs grew along one direction, which was parallel to the direction of the flow gas in the reaction system. Therefore, we infer that the orientation force for the growth of the long DWNT ropes is from the gas flow. Second, the ropes were continuous and very pure with less amorphous carbon and catalyst particles attached. They can be separated into several thinner ropes about 20 μm thick along the whole length without being broken. The continuous structure can be confirmed by another phenomenon: when attempting to break up and disperse the rope using a simple ultrasonication method in ethanol, the as-prepared rope was shrunk up, instead of broken up and dispersed, suggestive of their continuous structure and high purity. TGA and EDX results showed that the product contained 25% iron and 1.8% sulfur by weight, also indicating the good purity of the product.

Figure 1a shows an optical image of the as-prepared DWNT ropes. A low-magnification SEM image (Figure 1b) shows that an as-prepared DWNT rope with a thickness of about 15 μm is composed of thousands of roughly aligned filaments along its longitudinal direction. A high-magnification SEM image (Figure 1c) recorded over a single rope illustrates that it consists of well-aligned bundles of DWNTs, although a few bundles are also twisted with respect to the main rope, even forming some loop structures without a rupture, indicating their high flexibility and strength.

Polarized resonant Raman measurements can be performed to characterize the orientation of CNTs, due to their fundamental structural anisotropy.^{1,2,18} Previous research at a single nanotube level indicated that all modes reach their maximum intensity when the polarization of the incident laser is parallel to the nanotube axis, while normal to the nanotube axis they are

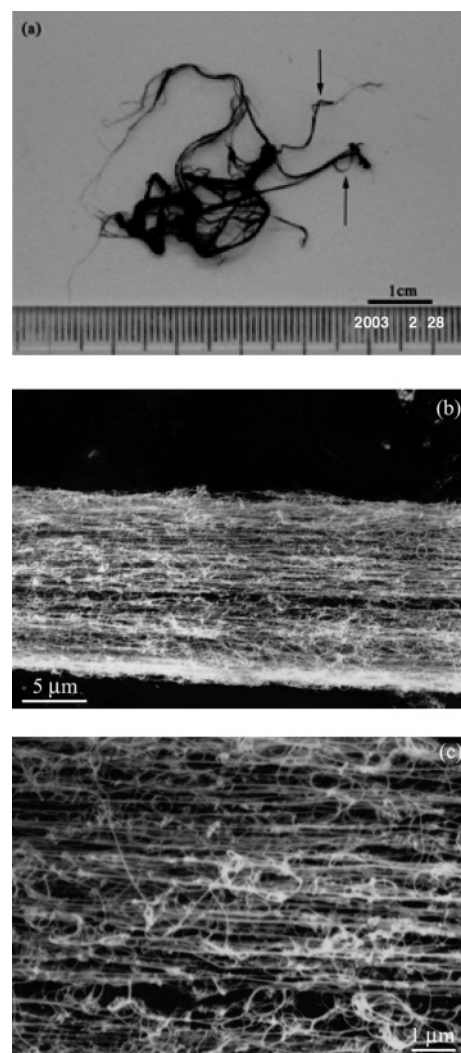


Figure 1. (a) Optical image of the as-prepared DWNT ropes. (b) Low-magnification and (c) high-magnification SEM images of a DWNT rope, respectively.

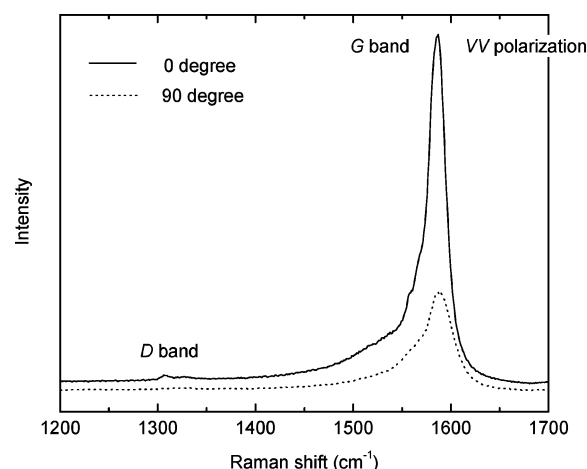


Figure 2. Polarized Raman spectra of a thin DWNT rope in the VV configuration. For $\theta = 0$ and 90° , the polarization of the incident laser is parallel and normal to the axis of the DWNT rope, respectively.

completely quenched due to the antenna effect.² Figure 2 shows a polarized resonant Raman spectrum recorded on an aligned DWNT rope. We found that the intensity of the G band, when the polarization of the incident laser was parallel to the nanotube axis, was about 4 times larger than that with the polarization of

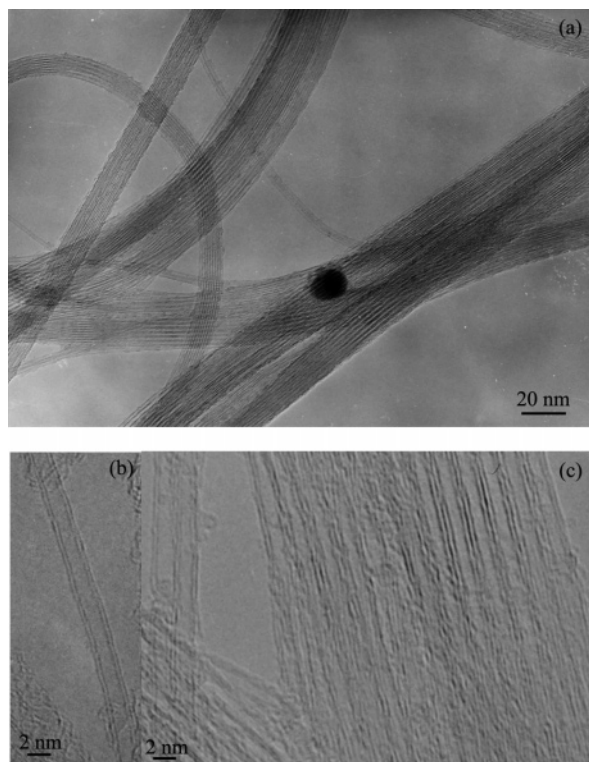


Figure 3. (a) Low-magnification TEM image of the as-prepared DWNT ropes. (b and c) HRTEM images of an isolated DWNT and several DWNT bundles in a rope, respectively.

the incident laser normal to the nanotube axis, indicating the alignment of the rope. However, when the polarization of the incident laser was normal to the nanotube axis, the *G* band still has a weak intensity rather than being completely quenched, as compared to the polarization study results reported on a single nanotube. We consider that this discrepancy may arise from the imperfect alignment of the rope, such as the twists and the loop structures of DWNT bundle, as shown in Figure 1c, since they can create other dipole fields to suppress the depolarization effect.² Moreover, it is worth noting that the *D* band exhibits a very small intensity relative to the *G* band, which also indicates the high quality of the as-prepared samples since the *D* band was considered to originate from the amorphous carbon in the samples and defects of carbon nanotubes.^{1,18}

Transmission electron microscopy (TEM) and high-resolution TEM (HRTEM) (Figure 3) were performed to gain insight into the further microstructural characteristics of the product. Note that the product has a high purity from low magnification TEM image (Figure 3a), in agreement with the SEM observations described previously. Moreover, many aligned DWNTs form some regular bundles with a thickness more than 20 nm due to the van der Waals attraction between the neighboring DWNTs. Figure 3b,c shows two typical HRTEM images of an isolated DWNT and several DWNT bundles. A great deal of HRTEM observations reveal that more than 90% of the product are DWNTs and their diameter distribution is much narrower (with diameter distribution width Γ of about 0.3 nm) than that of DWNTs reported before (Γ in the range of 1–3 nm),^{7–10} with outer and inner diameters of 1.7–2.0 and 1.0–1.3 nm, respectively. Sulfur was considered here to play an important role in the selective growth of DWNTs in the process by changing the activity of catalysts and consequently changing the decomposition of methane on the surface of catalysts since the shell numbers (1 or 2) of CNTs were related to the supply

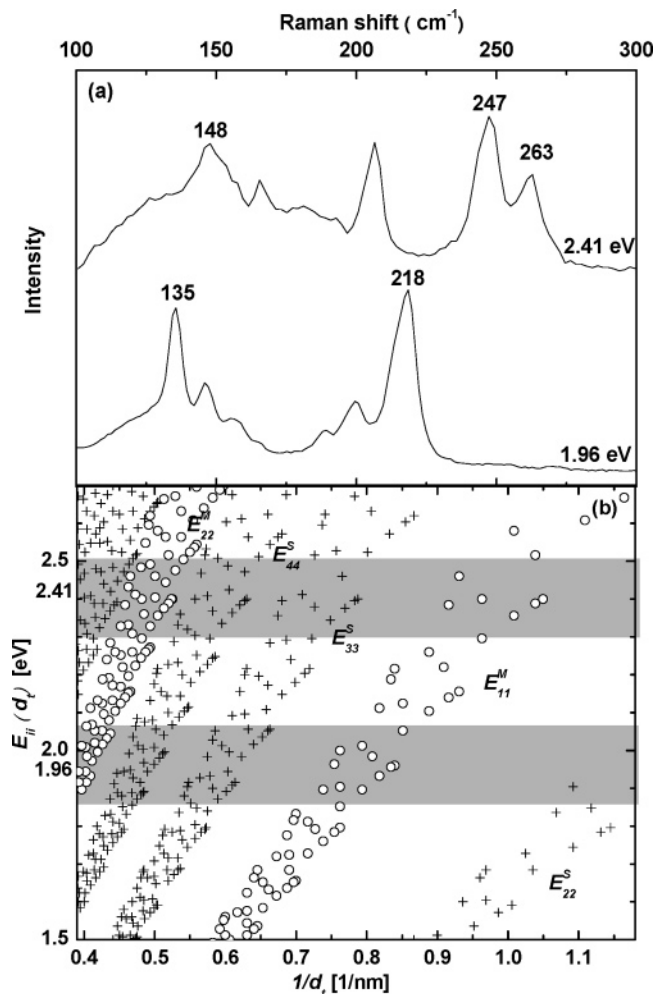


Figure 4. (a) RBM region of an as-prepared DWNT rope, excited by laser 632.8 and 514.5 nm, respectively. (b) Calculated energy separation E_{ii} as a function of $1/d_t$, $\gamma_0 = 2.90$ eV²⁴. Circles are for metallic SWNTs (E_{ii}^M), and crosses are for semiconducting SWNTs (E_{ii}^S). The two gray rectangular regions indicate the resonant windows 1.86 eV $< E_{ii} < 2.06$ eV and 2.31 eV $< E_{ii} < 2.51$ eV for the two excited lasers $E_{laser} = 1.96$ eV and $E_{laser} = 2.41$ eV, respectively.

of carbon to the catalyst particles with the same size, as reported by other groups.^{19,20}

Resonant Raman spectra provide an effective tool to detect the nanotube diameter since the electronic states are highly sensitive to the diameter of the nanotubes.^{1,2} Theoretical calculations showed that the radial breathing mode (RBM) frequency (ω_{RBM}) depends linearly on the reciprocal nanotube diameter d_t , with a relation $\omega_{RBM} = \alpha/d_t$.² Taking into account several influential factors about α , such as the tube wall curvature, intertube interaction, and interlayer interaction, $\alpha = 254$ cm^{−1} nm was performed to evaluate their diameters.⁸

Figure 4a shows two typical RBM spectra of the as-prepared DWNT ropes, excited by different lasers (632.8 and 514.5 nm, respectively). They mainly consist of two components at a low-frequency region forming pair peaks. The outer and inner diameters calculated using the relation $d_t = 254/\omega_{RBM}$ are roughly in the range of 1.7–2.0 and 1.0–1.3 nm, respectively. The difference in the mean diameter of the outer and inner diameter $\Delta \bar{d} = \bar{d}_{out} - \bar{d}_{in} \approx 0.74$ nm. The corresponding interlayer spacing (0.37 nm) is larger than the interlayer spacing of the graphite (0.335 nm), consistent with the HRTEM observations, which originates from the large repulsive force of the graphene basal planes between the adjacent small tubes, resulting from their large curvature.²¹

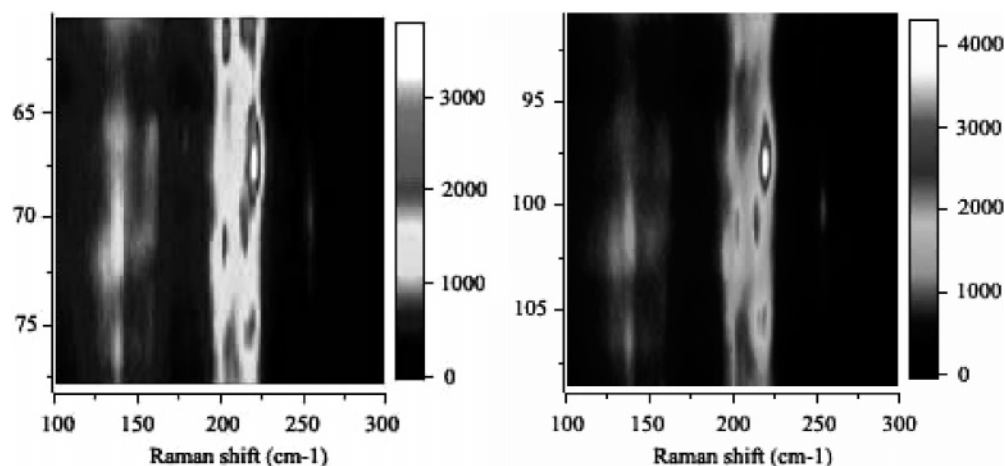


Figure 5. Raman images excited by a 632.8 nm laser, consisting of many Raman spectra recorded in a step of 0.5 μm along the directions parallel and perpendicular to the rope axis, respectively. The ordinate unit is μm , and the vertical color bar represents the intensity of Raman spectra.

To probe the homogeneity of the diameter of the product in a macroscopical scale, we recorded the spectra using 632.8 nm laser along the directions parallel and perpendicular to the rope, respectively, every half micrometer. The composed images (Figure 5) obtained showed that two narrow regions appeared in the RBM region with a Raman shift $< 20\text{ cm}^{-1}$ deviation from the center (135 and 218 cm^{-1}), corresponding to Γ smaller than 0.30 nm, in good agreement with the previous statistic data from HRTEM observations. This result indicates that the product has a very narrow diameter distribution in a macroscopical scale. Furthermore, we found that the intensity ratio of two maximum intensities ranged from 0.4 to 0.9. This result greatly deviates from the value (2:1) based on a lattice dynamical model under nonresonant conditions.²² We consider that this difference arises from two facts: (1) the Raman resonance cross-section decreases with increasing CNT diameter¹⁸ and (2) the different chirality combination of the two constituent tubes of a DWNT.^{8,23}

For some electronic applications, it is very important to identify the electronic properties of the constituent tubes of a CNT. For SWNTs, their electronic properties can be easily characterized by transport measurements, scanning tunnel microscopy (STM)/scanning tunnel spectroscopy (STS) analysis, and Raman measurements.¹ However, it is impossible to identify the electronic properties of the two constituent tubes of the DWNTs by the previous first two methods since only the outermost nanotube contributes to the STM image, STS conductance, and transport measurements.¹ Taking into account that the electronic structure of a DWNT can be understood by those of the two independent constituent SWNTs,^{1,3} and the combination of the corresponding double peaks in their Raman spectroscopy, it is possible to identify the electronic properties of the two constituent tubes by resonance Raman measurements. The resonance occurs for a particular diameter tube when the laser energy matches the electronic transition energy (E_{ii}) between van Hove singularities in the valence and conduction bands.² Therefore, the determination of the electronic properties of a nanotube by resonant Raman measurements depends primarily on the determination of E_{ii} and its diameter.

Figure 4b shows the diameter dependence of E_{ii} using $\gamma_0 = 2.90\text{ eV}$,^{2,24} where the E_{ii}^S for semiconducting tubes is indicated by the crosses and E_{ii}^M for metallic tubes by the open circles. The two gray rectangular regions show the resonant windows $1.86\text{ eV} < E_{ii} < 2.06\text{ eV}$ and $2.31\text{ eV} < E_{ii} < 2.51\text{ eV}$ for the two excited lasers $E_{\text{laser}} = 1.96\text{ eV}$ (632.8 nm) and $E_{\text{laser}} = 2.41\text{ eV}$ (514.5 nm), respectively. According to the resonant windows and the outer and inner diameters calculated, the electronic

properties of the corresponding tubes are identified. It is worth noting that the measured resonant Raman spectra in RBM region corresponding to the outer and inner tubes of the DWNTs in a rope were mostly generated from the resonant window E_{ii}^S and E_{ii}^M , respectively. That is to say, these resonant Raman spectra originate from the semiconducting and metallic tubes, respectively. These special DWNTs can be expected to be intriguing coaxial cables in nanoelectronic devices and nanocircuits.

Conclusion

In summary, we have shown a method for the direct synthesis of aligned DWNT long ropes with a narrow diameter distribution. The DWNT ropes are typically up to several centimeters in length and possess good alignment and high purity. HRTEM images and resonant Raman spectra indicate that the outer and inner tube diameters of the DWNTs are narrowly distributed in the range of 1.7–2.0 and 1.0–1.3 nm, respectively. Moreover, the electronic properties of the two constituent tubes of the DWNTs were identified based on the resonant Raman measurements, and the result indicates that the product consists of some semiconducting-metallic DWNTs. Such DWNTs provide a platform for fundamental studies and an ideal building block for applications in nanodevices.

Acknowledgment. The authors thank Drs. F. Li and P. H. Tan for useful discussions about polarization Raman measurements. The authors acknowledge NSFC grants (50025204 and 90206018) and the Special Fund for Major Basic Research Project (G2000026403) of MOST, China for support of this work.

References and Notes

- (1) Saito, R.; Dresselhaus, G.; Dresselhaus, M. S. *Physical Properties of Carbon Nanotubes*; Imperial College Press: London, 1998.
- (2) Dresselhaus, M. S.; Dresselhaus, G.; Jorio, A.; Souza, A. G.; Saito, R. *Carbon* **2002**, *40*, 2043.
- (3) Saito, R.; Dresselhaus, G.; Dresselhaus, M. S. *J. Appl. Phys.* **1993**, *73*, 494.
- (4) Saito, R.; Matsuo, R.; Kimura, T.; Dresselhaus, G.; Dresselhaus, M. S. *Chem. Phys. Lett.* **2001**, *348*, 187.
- (5) Zhang, S. L.; Liu, W. K.; Ruoff, R. S. *Nano Lett.* **2004**, *4*, 293.
- (6) Bandow, S.; Takizawa, M.; Hirahara, K.; Yudasaka, M.; Iijima, S. *Chem. Phys. Lett.* **2001**, *337*, 48.
- (7) Hutchison, J. L.; Kiselev, N. A.; Krinichnaya, E. P.; Krestinin, A. V.; Loutfy, R. O.; Morawsky, A. P.; Muradyan, V. E.; Obratsova, E. D.; Sloan, J.; Terekhov, S. V.; Zakharov, D. N. *Carbon* **2001**, *39*, 761.
- (8) Ren, W. C.; Li, F.; Chen, J.; Bai, S.; Cheng, H. M. *Chem. Phys. Lett.* **2002**, *359*, 196.

- (9) Ci, L. J.; Rao, Z. L.; Zhou, Z. P.; Tang, D. S.; Yan, Y. Q.; Liang, Y. X.; Liu, D. F.; Yuan, H. J.; Zhou, W. Y.; Wang, G.; Liu, W.; Xie, S. S. *Chem. Phys. Lett.* **2002**, 359, 63.
- (10) Li, W. Z.; Wen, J. G.; Sennett, M.; Ren, Z. F. *Chem. Phys. Lett.* **2003**, 368, 299.
- (11) Cheng, H. M.; Li, F.; Sun, X.; Brown, S. D. M.; Pimenta, M. A.; Marucci, A.; Dresselhaus, G.; Dresselhaus, M. S. *Chem. Phys. Lett.* **1998**, 289, 602.
- (12) Li, F.; Cheng, H. M.; Bai, S.; Su, G.; Dresselhaus, M. S. *Appl. Phys. Lett.* **2000**, 77, 3161.
- (13) De Heer, W. A.; Bacsá, W. S.; Chatelain, A.; Gerfin, T.; Humphrey-Baker, R.; Forro, L.; Ugarte, D. *Science* **1995**, 268, 845.
- (14) Kim, P.; Lieber, C. M. *Science* **1999**, 286, 2148.
- (15) Baughman, R. H.; Zakhidov, A. A.; De Heer, W. A. *Science* **2002**, 297, 787.
- (16) Ru, C. Q. *J. Appl. Phys.* **2000**, 87, 7227.
- (17) Cheng, H. M.; Li, F.; Su, G.; Pan, H. Y.; He, L. L.; Sun, X.; Dresselhaus, M. S. *Appl. Phys. Lett.* **1998**, 72, 3282.
- (18) Dresselhaus, M. S.; Eklund, P. C. *Adv. Phys.* **2000**, 49, 705.
- (19) Hafner, J. H.; Bronikowski, M. J.; Azamian, B. R.; Nikolaev, P.; Rinzler, A. G.; Colbert, D. T.; Smith, K. A.; Smalley, R. E. *Chem. Phys. Lett.* **1998**, 296, 195.
- (20) Flahaut, E.; Bacsá, R.; Peigney, A.; Laurent, C. *Chem. Commun.* **2003**, 1442.
- (21) Kiang, C. H.; Endo, M.; Ajayan, P. M.; Dresselhaus, G.; Dresselhaus, M. S. *Phys. Rev. B* **1998**, 81, 1869.
- (22) Popov, V. N.; Henrard, L. *Phys. Rev. B* **2002**, 65, 235415.
- (23) Charlier, A.; Mcrae, E.; Heyd, R.; Charlier, M. F.; Moretti, D. *Carbon* **1999**, 37, 1779.
- (24) Saito, R.; Dresselhaus, G.; Dresselhaus, M. S. *Phys. Rev. B* **2000**, 61, 2981.